Combination of Synchronous Condenser and Synthetic Inertia for Frequency Stability Enhancement in Low Inertia Systems

Nguyen, Ha Thi; Yang, Guangya; Nielsen, Arne Hejde; Jensen, Peter Højgaard

Published in:
I E E E Transactions on Sustainable Energy

Link to article, DOI:
10.1109/TSTE.2018.2856938

Publication date:
2018

Document Version
Peer reviewed version

This article has been accepted for publication in a future issue of this journal, but has not been fully edited. Content may change prior to final publication. Citation information: DOI 10.1109/TSTE.2018.2856938, IEEE Transactions on Sustainable Energy

Combination of Synchronous Condenser and Synthetic Inertia for Frequency Stability Enhancement in Low Inertia Systems

Ha Thi Nguyen, *Student Member, IEEE,* Guangya Yang, *Senior Member, IEEE,* Arne Hejde Nielsen, *Senior Member, IEEE,* and Peter Højgaard Jensen

***Abstract*—Inertia reduction due to high-level penetration of converter interfaced components may result in frequency stability issues. The paper proposes and analyzes different strategies using synchronous condenser (SC), synthetic inertia (SI) of wind power plant, and their combination to enhance the frequency stability of low inertia systems under various scenarios and wind conditions. Furthermore, one of the SC models includes hardware of automatic voltage regulator (AVR) for better representation of the reality is implemented. The simplified Western Danish power system simulated in real time digital simulator (RTDS) is used as a test system of low inertia to demonstrate the effectiveness of the strategies. The comparative results show that the combination of SC with AVR hardware-in-the-loop test and SI offers a better improvement not only on frequency stability (rate of change of frequency and frequency deviation) but also on the system synchronism under various operating conditions.**

***Index Terms*—Frequency stability, low inertia systems, synchronous condenser, synthetic inertia, wind power.**

I. Introduction

WITH the replacement of conventional generation by power electronic-based generation such as wind power plants, photovoltatics plants, and importing high-voltage direct current (HVDC) links, the significant inherent rotational inertia property of traditional power plants is displaced by a smaller or no rotational inertia of converter interfaced generation. Therefore, high-level power electronic-based generation penetration makes the system inertia reduce that leads to the system frequency more vulnerable and probable frequency instability under severe disturbances.

There have been many researchers considering the impact of low inertia on power system stability and operation because of high renewable energy penetration level [1]–[3]. In [1], a research related to system inertia and the challenge in the system operation due to the inertia reduction are investigated. The study proposes using storage devices or inertia of converter connected generation as a solution for low inertia systems. Maintaining sufficient inertia in the system to guarantee operational security is a main challenge of the Nordic power system [2]. The low inertia effect on power system operation and stability with high converter-connected wind turbine and photovoltaic penetration level is analyzed in [3]. The paper demonstrates that system inertia becomes heterogeneous and frequency dynamics are faster in power systems with low inertia. Recently, 1200 MW photovoltaic resource interruption incident in the Southern California system is occurred due to low system frequency condition that activates inverters trip based on the instantaneous frequency measurement during a fault [4]. Consequently, the low inertia issue has been generally recognized.

To improve the frequency stability, transmission system operators (TSOs) have issued grid codes to the participation of wind power plants (WPPs) in frequency control [5]. In addition, the role and potential ability of WPPs for supporting frequency control have been investigated in [6] that provides foreseeable ideas for further research work on WPPs. Recent literature proposed strategies on implementing inertial support of WPPs, the so-called synthetic inertia (SI), most of them propose a supplementary control into active power loop that is activated during frequency changes. It can be classified into two main categories. The first one attempts to mimic the inertial response of conventional power plants [7], [8] that uses df/dt as an input signal, while the second one takes frequency deviation as an input signal with fast response time [9], [10]. The authors in [11] use the combination of the two control strategies to provide inertial response for WPP. An ancillary control signal proportional to df/dt and frequency deviation is used to increase/decrease the electric power of WPP.

A number of authors have paid more attention to the activation schemes instead of control methods for SI implementation [12], [13]. A coordination of inertial response and grid event detector using a demanded inertia response and df/dt calculation trigger are studied in [12], whereas different activation methods are proposed and analyzed in [13] that focuses on trigger schemes without coordinated with the control. Based on the above-mentioned literature, a fulfilled control strategy investigated both the control method and the activation scheme for SI of WPPs has not done yet. Moreover, the synthetic inertia from WPPs is not fast enough to react in severe disturbances.

Synchronous condenser (SC) has been playing an important role in reactive power compensation and keeping voltage stability in power systems for a couple of decades [14]. By varying the field excitation current, SC can operate at over-excited or under-excited modes to supply/absorb reactive power to/from the network that can control smoothly the

H. T. Nguyen, G. Y. Yang and A. H. Nielsen are with the Center for Electric Power and Energy, Department of Electrical Engineering, Technical University of Denmark, Kongens Lyngby, DK-2800, Denmark (e-mail: (thangu, gyy, ahn)@elektro.dtu.dk, nthadht@gmail.com)

P. H. Jensen is with Energy Automation, Siemens A/S, 2750 Ballerup, Denmark (e-mail: peter_hoejgaard.jensen@siemens.com)

This article has been accepted for publication in a future issue of this journal, but has not been fully edited. Content may change prior to final publication. Citation information: DOI 10.1109/TSTE.2018.2856938, IEEE Transactions on Sustainable Energy

voltage or keep the system power factor at a specified level. SC can also support the short-circuit power to the network that can improve system interconnections, facilitates system protection and enhances the operation of modern power electronics installations [15]. Furthermore, using SC for decreasing under frequency load shedding is investigated in [16] and a interaction between active power and reactive power channels of synchronous condensers to improve primary frequency control is studied in [17].

Completely different from WPPs, SC is an alternator that can provide inherently inertial response due to the electromechanical coupling with the grid. The kinetic energy stored in its rotating mass can naturally counteract the frequency change during disturbances.

From the literature review, the difference between SC and SI in terms of frequency support is not very well clarified. In this paper, synchronous condenser and SI of WPPs are investigated and clearly shown for the frequency stability improvement of low inertia systems. Firstly, usage SC providing the inherent rotating energy to support inertial response that helps primary control has more time to react during system frequency changes. The SC model includes a real automatic voltage regulator (AVR) system that is interfaced with the simulation through hardware-in-the-loop (HiL). HiL provides an efficient real-time control and a safe environment where tests can focus on the functionality of the controller and verify all dynamic conditions of the system, which is hard to implement in real devices [18], [19]. During HiL test, the physical system of AVR interfaces with the rest of SC and the grid that are simulated in real-time digital simulator (RTDS), and the outputs of the simulation imitate the actual output of the physical AVR system. Secondly, a SI controller of WPPs and its activation scheme are proposed. The difference of inertia characteristic between SC and SI for the frequency control is analyzed. Finally, a combination of SC and SI is examined that shows a better performance not only in frequency stability enhancement but also in system frequency synchronism. These methods are demonstrated on the future Western Danish renewable-based (DK1) system to analyze their performance during disturbances. Different scenarios and wind speed conditions are investigated to examine the effectiveness of these approaches.

The remaining part of the paper is organized as follows. Section II introduces the system configuration, system frequency characteristics, SC with AVR HiL testing, and control design for SI of WPPs. The comparative results of different scenarios and wind speed conditions using various strategies are analyzed and discussed in section III. Some specific important conclusions are drawn in section IV.

II. Frequency Stability Enhancement Using SC and SI of WPPs

In this section, the system configuration of DK1 system that is used as a low inertia system background is firstly depicted. After that, the system frequency characteristic is clearly analyzed. Finally, the AVR HiL testing model of SC and control design for SI of WPPs are investigated.

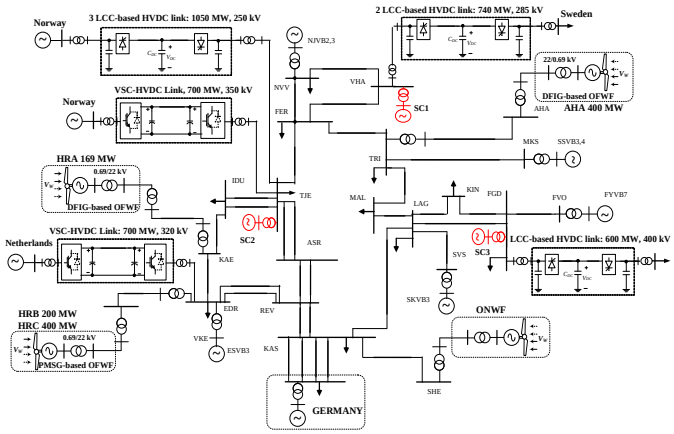

Fig. 1. Single-line diagram of 400 kV Western Danish renewable-based system in 2020.

A. System Configuration

Fig. 1 shows the DK1 system in 2020 that is using a majority of renewable energy and interconnecting to the neighboring countries through HVDC links. This system is based on the current DK1 system [20] adding more 400 MW offshore wind farm (HRC or HR3) and 700 MW Voltage-sourced converter (VSC) HVDC interconnection to the Netherlands (COBRA cable) that are operating in 2017 and in 2019, respectively. The German grid is modeled by a large synchronous generator with 7 s inertia constant and a load. The frequency control support of the German grid is adjusted proportional to the power exchange. There are three synchronous condensers (the marked red in Fig. 1) connected at three line-commutated converter (LCC) HVDC terminals with the detail parameters in Table I. The AVR of synchronous condenser located at bus FGD uses real control system to evaluate its performance during disturbances. There are three aggregate offshore wind farms (OFWFs), and one aggregate onshore wind farm (ONWF) as shown in Fig. 1.

TABLE I
Synchronous Condenser Parameters.

SCs	Location	S_{rated} (MVA)	V_{rated} (kV)	Q_{min} (Mvar)	Q_{max} (Mvar)	H (s)
SC1	VHA	200	12	-100	150	2
SC2	TJE	250	13	-120	200	2.2
SC3	FGD	270	15.75	-144	242	2.5

B. System Frequency Characteristics

Inertia is defined as the resistance of a physical object to changes in its state and position, consisting of its speed and direction [1]. Applying to an electrical power system, the physical objects are the rotating machines (generators, motors, etc.) connected directly to the power system and the resistance to the change in rotational speed is expressed by the moment of inertia of their rotating mass. It is assumed that only synchronous machines (generator and condenser) contribute to the system inertia in the respect of physics. The

This article has been accepted for publication in a future issue of this journal, but has not been fully edited. Content may change prior to final publication. Citation information: DOI 10.1109/TSTE.2018.2856938, IEEE Transactions on Sustainable Energy

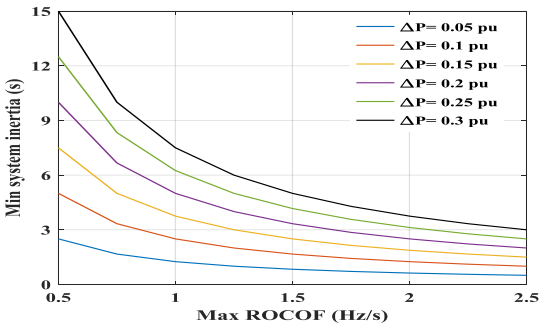

Fig. 2. The dependence of system inertia on maximum ROCOF and disturbance size.

system inertia of a power system is referred to the nominal apparent power of synchronous machines that is defined by

$$H_{sys} = \frac{\sum_{i=1}^{N} (S_{ni} H_i)}{S_{sys}} \tag{1}$$

where S_{sys} is selected equal to the total load of system; N is the number of synchronous machines; and S_{ni} and H_i are the nominal apparent power and the inertia constant of i-th synchronous machine, respectively. The system inertia depends on the number of operating rotating machines and the inertia constant of each machine.

A sudden change in load or generation causes a change in the generation-demand equilibrium. The system inertia constant plays a vital role in the first few seconds, after that primary control picks up the frequency deviation by controlling the governor to return the frequency to acceptable operating value within 30 s. A higher inertia constant results in a lower rate of change of frequency (ROCOF), which gives time to the primary control regulating the power output.

The initial ROCOF that is determined by the size of the power imbalance and the system inertia is expressed by

$$ROCOF = \frac{f_0}{2H_{sys}} \frac{\Delta P}{S_{sys}} \tag{2}$$

where ΔP is the disturbance size; f_0 is the nominal system frequency. Let define H_1 and $ROCOF_1$ are the system inertia and ROCOF of the current system, and H_2 and $ROCOF_2$ are those of the future system that uses a majority of renewable energy, respectively. Hence, ROCOFs of these two systems for a given disturbance are described based on (2) as follows:

$$ROCOF_1 = \frac{f_0}{2H_1} \frac{\Delta P}{S_{sys}} \tag{3}$$

$$ROCOF_2 = \frac{f_0}{2H_2} \frac{\Delta P}{S_{sys}} \tag{4}$$

From (3) and (4) gives:

$$H_2 = H_1 \frac{ROCOF_1}{ROCOF_2} \tag{5}$$

From (5), when the maximum ROCOF that is imposed by TSOs is set, the minimum system inertia of the future system for a given disturbance is determined based on the current system, which beyond it ROCOF of the future system would be over the permissible value. The minimum system inertia enables the system withstand a certain disturbance without exceeding a certain ROCOF is shown in Fig. 2. The general evaluation of minimum inertia will cover disturbance size from 5% to 30% of the system load, and maximum ROCOF between 0.5 and 2.5 Hz/s [21]. As can be seen clearly that there is a reverse correlation between minimum system inertia and maximum ROCOF, the higher maximum ROCOF is allowed, the lower minimum system inertia is required. On the contrary, a positive one exists between minimum system inertia and disturbance size, a larger disturbance requires a higher system inertia in order to the system frequency is not over the permissible maximum ROCOF.

The frequency deviation is regulated by the available frequency containment reserves. In the test system, it depends on the available primary control headroom of the online synchronous generators (SGs) and the German grid. The Western Danish system is synchronized to the Continental European system where its primary reserve is designed in order to the system frequency deviation remains within a certain range for ordinary as well as severe contingencies [22].

The system primary regulation constant for the entire system in MW/Hz is determined by

$$K_{sys} = \sum_{i=1}^{N} K_i = \sum_{i=1}^{N} \frac{S_{ni}}{R_i f_0} \tag{6}$$

where K_i and R_i are regulation constant and droop gain of i-th synchronous generator, respectively. The system primary regulation constant determines how much active power supplies/absorbs against frequency changes. K_{sys} is normally kept fix and decided by the primary reserve.

When the system operates with high renewable energy production, high importing HVDC links, and phasing out of conventional power plants, the system inertia reduces significantly that makes the frequency dynamics faster and more vulnerable. This may result in an activation of under frequency load shedding or ROCOF-operated protection relays for tripping transmission lines. As a result, the system freely gets split and more challenging to operate. Cascading failure or even system blackout may therefore occur. In the low inertia operating situation, some possible solutions TSOs could be implemented in form of grid codes such as the minimum system inertia requirement, limiting the power output of large importing HVDC interconnections, or HVDC emergency power control to guarantee for the operational stability of the system.

Regarding the load model, the lately proposed Western Electricity Coordinating Council (WECC) composite load model can better represent the dynamic behavior of loads during faults [23-24], which is the advantage of WECC model compared to static load models. However, the inertia of the motor in the model may not represent the worst case for the frequency stability study. Therefore, the paper uses the ZIP load model instead, where the parameters of the model are based on the information provided by the operators. A ZIP load model as a function of frequency variation and voltage magnitude that is called voltage & frequency dependent load

This article has been accepted for publication in a future issue of this journal, but has not been fully edited. Content may change prior to final publication. Citation information: DOI 10.1109/TSTE.2018.2856938, IEEE Transactions on Sustainable Energy

(V&FDL) model is implemented in this paper, yielding to the following equation

$$P_L = P_0(1 + k_{Pf}\Delta f)(p_p + p_c\frac{V}{V_0} + p_z(\frac{V}{V_0})^2) \quad (7)$$

$$Q_L = Q_0(1 + k_{Qf}\Delta f)(q_p + q_c\frac{V}{V_0} + q_z(\frac{V}{V_0})^2) \quad (8)$$

where P_L and Q_L are the active power and reactive power of the load (pu); P_0 and Q_0 are the rated active power and reactive power of the load (pu); V_0 and V are the nominal and actual voltage magnitude at the load bus (pu); f_0 and Δf are the nominal frequency and frequency deviation (pu); k_{Pf} and k_{Qf} are the frequency characteristic coefficients; p_p and q_p are the portion of total load proportional to constant active power load; p_c and q_c are the portion of total load proportional to constant current load; p_z and q_z are the portion of total load proportional to constant impedance load, respectively.

C. AVR hardware in the loop for synchronous condenser

The AVR of the biggest capacity SC (SC3) located at bus FGD is implemented HiL, whereas the other ones use modified IEEE standard model of AC7B excitation system, which is included in the RTDS library to have a similar response with the AVR used in HiL.

The entire grid and SC model are simulated in RTDS with the dash blue bound, while AVR system is implemented HiL with the dash red one as shown in Fig. 3. RTDS sends three-phase currents and voltages of the SC terminal, as well as the frequency and voltage measured at the busbar to AVR, whereas AVR set point (AVR SP) is sent to RTDS.

The AVR is implemented based on PID controller of the AVR system of IEEE AC7B excitation model as shown in Fig. 4 that is modeled in VisSim software in PC1 and then programmed on PLC S7-400. Furthermore, S7-400 integrates with supervisory control and data acquisition (SCADA) system on PC2 using WinCC via IEC 104 standard for continuous monitoring, data storage, control, and analysis. The SC behavior can be captured over a long real-time period and used for further analysis.

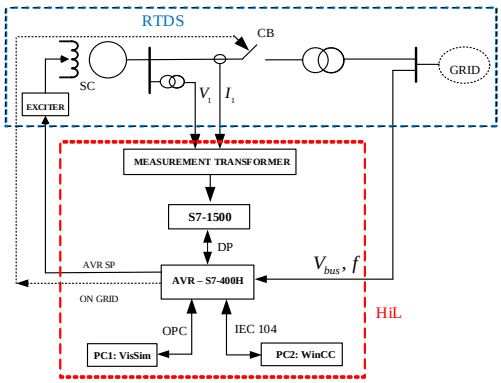

Fig. 3. Hardware in the loop testing setup for AVR system.

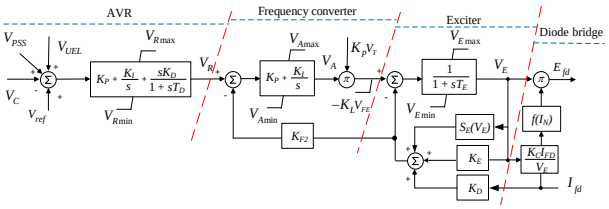

Fig. 4. IEEE AC7B excitation system.

D. Synthetic inertia of WPPs

Because the replacement for traditional generation by renewable-based generation may results in more challenging for the system frequency stability, TSOs have issued grid codes to all grid-connected generators. For instance, WPPs with rated power above 10 MW in the UK, above 50 MW in the continental European grid, and above 5 MW in Ireland must be equipped with a control system for frequency response [5], [25]. To satisfy the grid connection requirement, SI controller for WPPs that mimics the inertial response behavior of the conventional power plant during power imbalances is extremely necessary.

Fig. 5 shows the proposed synthetic inertia controller that includes two control loops, the first one takes df/dt as the input to create an additional signal T_1, the second one generates an extra signal T_2 from frequency deviation input. In order to avoid competing control effect, the proposed method switches the reference from T_{ref} of MPPT control to T_{SI} of the proposed scheme during the inertia response. The output of SI can be expressed as follows:

$$T_{SI} = K_{in}\frac{df}{dt} - K_{droop}\Delta f + T_{refp} \quad (9)$$

where T_{refp} is the reference from MPPT corresponding to pre-disturbance rotor speed that is stored on the system data.

A low-pass filter is used to eliminate the measurement noise. Furthermore, a dead band (± 0.015 Hz) is deployed to avoid the participation of the synthetic inertia control on a small frequency variation. A high-pass filter (HPF) is applied to guarantee that the Δf control loop does not contribute when the system frequency reaches a new equilibrium and the turbine can recover the operating speed.

It is important to select properly the values of K_{in} and K_{droop}. Otherwise, it may cause a poor performance for the controller. K_{in} is proportional to df/dt control loop, a high K_{in} value may result in over ramping up limit of turbine speed that can destroy the mechanical part of turbine. K_{droop} is the gain of Δf control loop, a high K_{droop} selection may

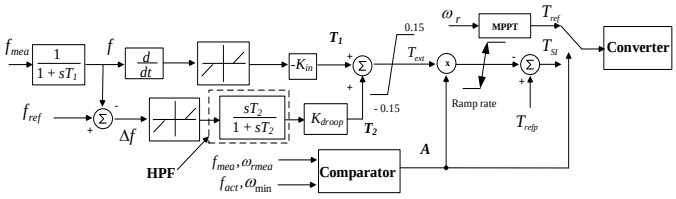

Fig. 5. Synthetic inertia controller of WPP.

This article has been accepted for publication in a future issue of this journal, but has not been fully edited. Content may change prior to final publication. Citation information: DOI 10.1109/TSTE.2018.2856938, IEEE Transactions on Sustainable Energy

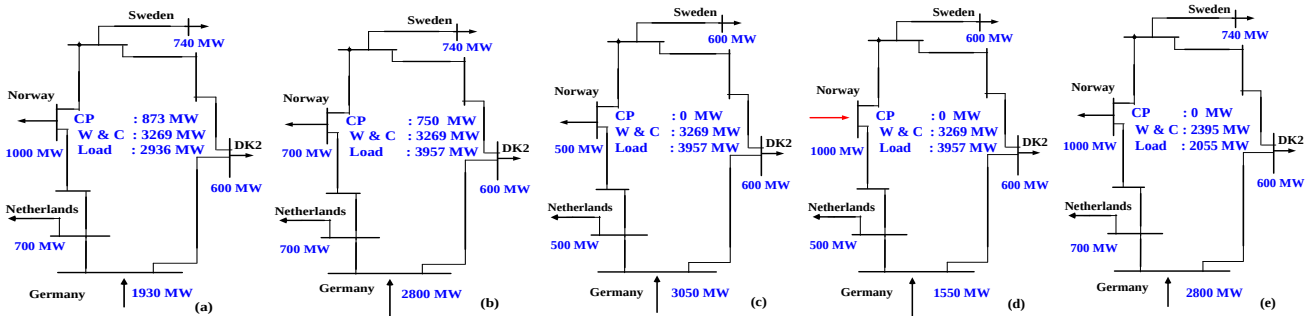

Fig. 6. Case-study scenarios (CP: central production, W & C: wind and coastal production). (a) Base case. (b) HLHW with 3 SGs. (c) HLHW no SGs, exporting to Norway. (d) HLHW no SGs, importing from Norway. (e) LWLL.

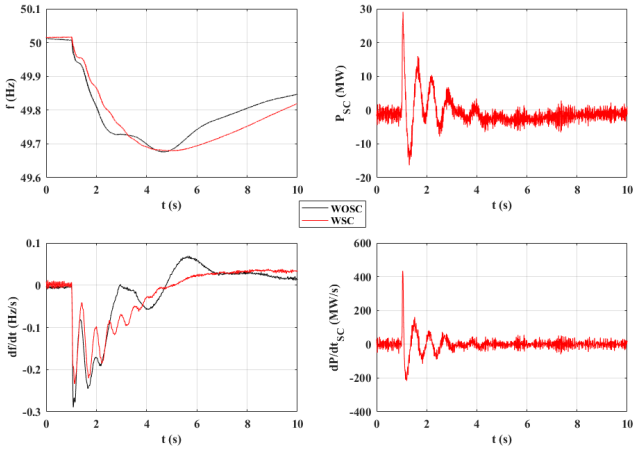

Fig. 7. System frequency, ROCOF, and SC responses during a disturbance of base case.

lead to the large turbine speed drop that makes the turbine cannot recover the operating point after disturbances. K_{droop} is selected based on the droop characteristics of SG (from 2%-12%) [5]. An optimal combination of the two gains can obtain a good performance for SI on the frequency stability improvement [26].

An activation scheme combined with a minimum rotor speed check is implemented on this control strategy to make sure that the rotor speed does not operate below its the minimum speed limit that may stall the turbine. The activation scheme can be described by

$$if \begin{cases} f_{\min} \le f_{mea} \le f_{\max} \\ \omega_{rmea} \le \omega_{\min} \end{cases} : setA = 0 \qquad (10)$$
$$else: setA = 1$$

SI controller is implemented for the three OFWFs of the system, one PMSG-based OFWF, and two DFIG-based OFWFs, as shown in Fig. 1. A ramp rate limit ($\pm$ 0.5 pu/s) is added to prevent the immediate on/off activated signal in case reaching the minimum allowable rotor speed limit. A proper value of the ramp rate limit makes the transfer period smoother and less mechanical stress on the turbine and rotor that is discussed in the result section.

III. Case Studies

Different scenarios and wind speed conditions are investigated in order to examine the proposed method under various disturbances/faults.

A. Base case

The case is based on the DK1 system data in 2020, all 5 local SGs (873 MW central production) are operating with the detail data as shown in Fig. 6(a).

In order to verify the contribution of SC to the frequency stability improvement, the system response during 200 MW load located at MAL increases at t = 1 s with and without SC is shown in Fig. 7. With SC the system frequency is much smoother and stronger while ROCOF is lower than that of without SC: nearly 0.29 Hz/s versus around 0.233 Hz/s, that are quite accurate with the Matlab calculation based on (2) as shown in Table II. It is noteworthy that when the disturbance occurs SC simultaneously supplies the electric energy to the system to against the frequency drop with nearly 420 MW/s active power gradient. With HiL test of AVR, AVR in HiL will update the changes of voltage and current measurement of SC to calculate AVR SP and send back to SC in RTDS to control the terminal voltage during the disturbance. It can be seen that SC can improve significantly ROCOF of the system thanks to the swiftly rotating energy supply to the inertial response.

B. High wind and high load (HWHL)

1) High wind and high load with 3 online SGs: In this scenario, the load capacity is simulated for the future load (in 2050) that is estimated 1% increase per year based on the base case load and the wind speed condition reaches the rated speed at 12 m/s so that WPPs are operating at their rated power output. The system data with three committed SGs is shown in Fig. 6(b).

The system responses during 10% of the total current load located at bus MAL increases at t = 2 s are illustrated in Fig. 8. The black line represents the system responses without SC and SI implementation, while the red one and blue one describe the system responses with SI and with SI combined SC, respectively. With SI controller the frequency nadir is significantly enhanced from around 49.48 Hz to 49.55 Hz while ROCOF is slightly improved. An opposite correlation

This article has been accepted for publication in a future issue of this journal, but has not been fully edited. Content may change prior to final publication. Citation information: DOI 10.1109/TSTE.2018.2856938, IEEE Transactions on Sustainable Energy

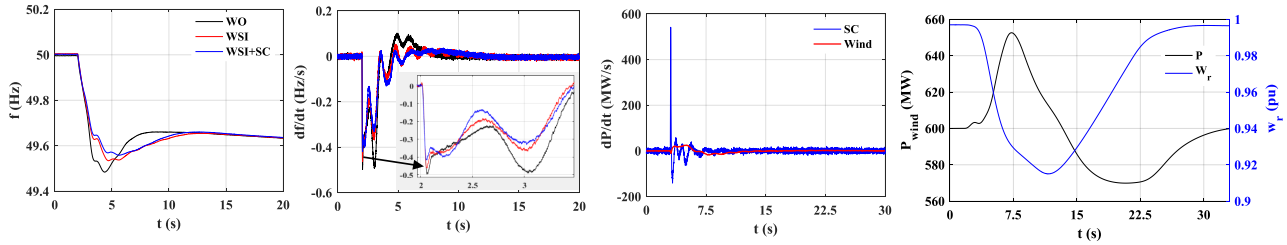

Fig. 8. System responses during a 10% load increase disturbance of HWHL 3 SGs in operation.

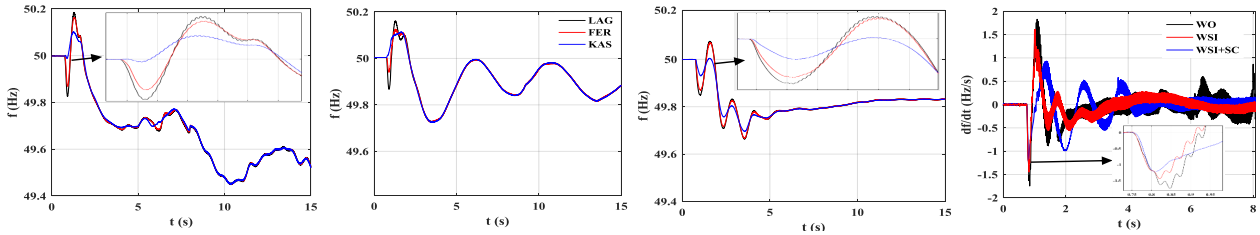

Fig. 9. System responses during a 10% load increase disturbance of HWHL no local SGs in operation WO, WSI, and WSI+SC.

is seen when SCs are in service, ROCOF is drastically decreased from 0.5 Hz/s to approximately 0.4 Hz/s, whereas the frequency nadir has a small improvement. It can be explained that when the disturbance occurs, at first few second SC's rotating energy is released in order to support to system inertial response that helps ROCOF improve, SI responds afterwards to increase temporarily WPP power output counteracting the frequency drop as well as compensate for SC's rotating energy. It can be seen much more clearly about the response time that shows how fast they react from the active power gradient (dP/dt) plots of SC and WPP in Fig. 8. Consequently, the combination of SI and SC results in an efficient enhancement of the frequency stability in term of frequency nadir and ROCOF. As expected, WPP can recover the pre-disturbance operating speed when the system frequency reaches a new equilibrium.

2) High wind and high load without online SGs: In this scenario, the system operates without any local committed SGs (no central production) with the power flow as shown in Fig. 6(c). In order to support the inertial response, three more SCs are installed to the system at KAS, TRI, and EDR that are the same specification with SC3. The locations of SC installation are based on the reactive power support demand through power flow calculation. In this situation, the system operates in a very low inertia constant and relies largely on the German interconnection. The frequency is measured at three locations KAS, LAG, and FER to witness the frequency synchronization when the system operates in a low inertia condition.

Load increase disturbance: The same load increase disturbance size occurs. As can be seen clearly from Fig. 9 that the system frequency without SCSI (WO) undergoes a huge oscillation and gets unstable after around 5 s because only the German side inertial support is not enough for the frequency recovery. An interesting point should be mentioned here is the various frequency behavior in different parts of the system. A reverse oscillation occurs with the frequency at KAS compared to that of FER and LAG. With the combination of SC and SI, the system stays in synchronism and becomes stable after approximately 5 s as seen in the third sub-plot. It can be explained that at the first few seconds, the inertial response mainly from the German side and SCs tries to restrain the frequency change, after that the inertia support from SI of WPPs and primary control help the system frequency recovery and stable. Only SI in operation is not fast enough for the frequency support in this low inertia condition, which leads to a large oscillation before getting stable on the frequency, as shown in the second sub-plot of Fig. 9.

A three-phase short circuit: A three-phase short-circuit fault occurs at t = 1.6 s and cleared at t = 1.7 s at the bus TRI, and after that the circuit breaker of TRI load (250 MW) is activated to disconnect the load. The comparative results suggest that with SCSI not only the frequency stability is improved significantly, but also the system is much more synchronized (Fig. 10(a)). Without any inertia supports of SC and SI, the frequency experiences a huge deviation and ROCOF reaches around 3.5 Hz/s. A significant enhancement of maximum frequency and oscillation damping is observed when SIs are in service. The maximum frequency is reduced considerably and rapidly settles down without further increase like the WO case. On the other hand, a huge enhancement is observed in ROCOF with SC in operation. However, a quite large frequency deviation is witnessed with SC after the TRI load disconnection. This can be explained that at the first few seconds following the fault, the German side and all of SCs inherently contribute inertial response to the grid by absorbing the power to against the frequency increase that can be observed in a significantly ROCOF improvement. After supporting inertial response, SCs release the energy to the grid to recover their speed which makes the frequency deviation larger as shown in Fig. 10(a). This issue is addressed with the combination of SC and SI in operation. ROCOF is lower from nearly 3.5 Hz/s (WO) to 2.5 Hz/s that satisfies the acceptable range of the Continental European grid code ($\pm$ 2.5 Hz/s) [27].

This article has been accepted for publication in a future issue of this journal, but has not been fully edited. Content may change prior to final publication. Citation information: DOI 10.1109/TSTE.2018.2856938, IEEE Transactions on Sustainable Energy

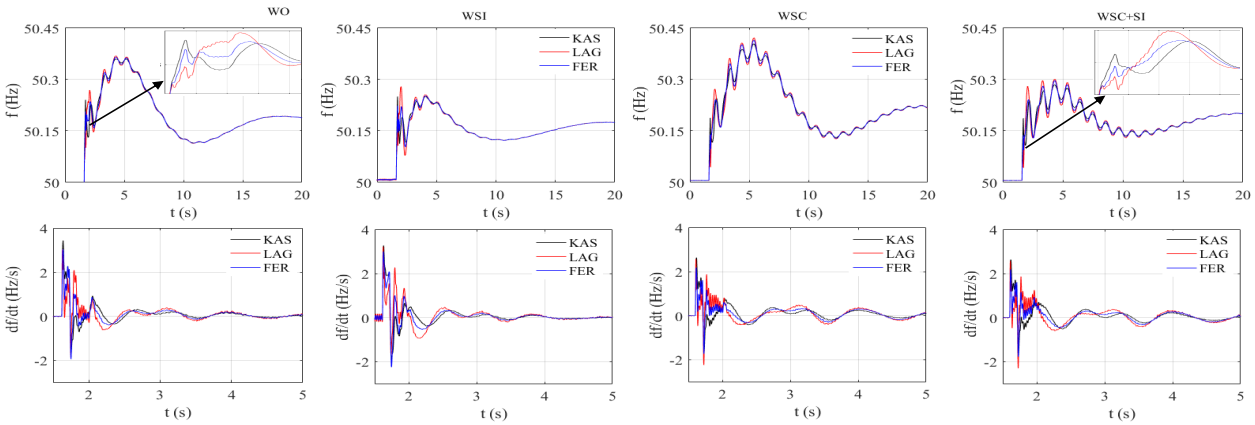

(a) Exporting HVDC link to Norway.

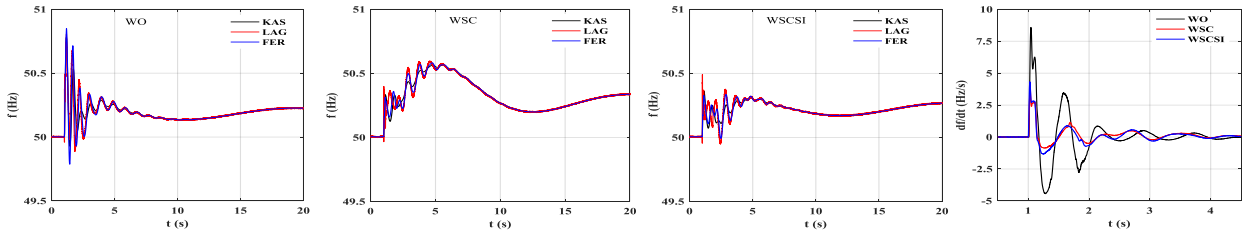

(b) Importing HVDC link from Norway.

Fig. 10. System frequency and ROCOF during a three-phase short-circuit fault with WO, WSI, WSC, and WSC+SI.

Another scenario of HWHL without online SGs is switching the power transfer direction of HVDC links to Norway. The current power flow of the system is listed detail in Fig. 6(d). The 1000 MW power is imported from Norway to DK1 through HVDC links, which leads to a reduction in importing power and the frequency control support from the German grid. Consequently, the system frequency dynamics is faster, the frequency deviation and ROCOF are much larger than the exporting HVDC links from Norway case with the same incident sequence at bus TRI as shown in Fig. 10(b). Specially, ROCOF that is measured at bus KAS even reaches approximately 8.5 Hz/s instead of 3.7 Hz/s in the previous one. With SC and SI are in service, this value is considerably enhanced around 4.3 Hz/s. However, this value is out of the acceptable range of the grid code ($\pm$ 2.5 Hz/s), a limit of power output of importing HVDC link, or system inertia minimum requirement, or more synchronous condenser installations should be implemented in low inertia systems.

C. Low wind and low load (LWLL)

This scenario examines the SI controller operating in low wind speed condition (V_W= 9.5 m/s) that leads to the rotor speed hit its minimum allowable speed during a disturbance. The system operates with 70% of the base case load and no central production with the detail data as shown in Fig. 6(e). In this scenario, DK1 system operates like a corridor to transfer the power from Germany to Norway, Sweden, and the Netherlands.

As expected, the ROCOF experiences a 0.2 Hz/s improvement from -0.6 Hz/s to -0.4 Hz/s when SCs are in operation during 15% current load increase disturbance as shown in Fig. 11. On the other hand, the frequency nadir and settling time have a significant enhancement with SI controller. It is noteworthy that (2) is not precise in low inertia systems as shown in Table II.

An interesting point which should be concerned here is the rotor speed hits the minimum speed limit that is set 0.75 pu during the disturbance. This causes an unsmooth response on the recovery section of the active power and the rotor speed. It is worth to mention that a proper ramp rate limit can help the rotor speed response smoother and reduce the mechanical stress.

A comparative load behavior of frequency dependent load (FDL) and V&FDL of FER load is shown in the last sub-plot of Fig. 11. It can be seen that the load changes immediately after the onset of the disturbance and is mainly caused by the voltage dependence.

IV. Conclusion

With a sharp increase of converter-based generation in power system, there is a significant reduction on the system inertia and the primary frequency control. That may cause a faster frequency dynamics and a larger frequency deviation. Additionally, the system inertia constant becomes time-variant because of the variability of power dispatch and demand scenarios.

The paper proposes different strategies for frequency stability improvement that use SC, SI of WPP, and their combination to support the inertia response for the low inertia system during power imbalances and three-phase short-circuit fault. In addition, hardware-in-the-loop test of AVR is implemented to validate its controller before deployment.

This article has been accepted for publication in a future issue of this journal, but has not been fully edited. Content may change prior to final publication. Citation information: DOI 10.1109/TSTE.2018.2856938, IEEE Transactions on Sustainable Energy

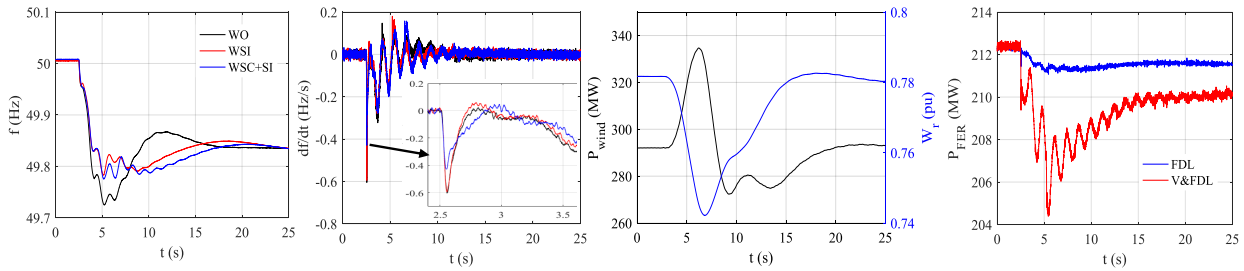

Fig. 11. System responses during a disturbance of LWLL.

The combination of SC and SI may pronounce the inertial response of a synchronous generator during a frequency excursion. The inertial response is from SC mainly improving ROCOF, afterwards the primary frequency control with fast time response from SI of WPPs takes over and significantly enhancing frequency deviation. This work is based on the simulation to show how to tune K_{in} and K_{droop} to adjust the output of WPP to support frequency stability and compensate the kinetic energy recovery of SC after its inertial response to help the system quickly settle down. K_{in} is tuned to get a proper power at the beginning of the SI response based on df/dt whereas K_{droop} and T_2 are tuned based on frequency deviation to adjust how large and fast the output of SI is. As a result, a combination of SC and SI provides a better performance that not only enhances maximum/minimum frequency and ROCOF, but also helps the low inertia system more synchronized during different disturbances. Furthermore, TSOs may impose requirements on the minimum system inertia and examine the impact of HVDC in low inertia operating conditions.

TABLE II
SYSTEM INERTIA AND ROCOF IN MATLAB CALCULATION.

-	Cases	(a)	(b)	(c)	(e)
H (s)	WOSC	6.53	5.42	4.54	8.76
	WSCs	7.46	6.1	5.52	10.63
ROCOF (Hz/s)	WOSC	-0.26	-0.45	-0.56	-0.43
	WSCs	-0.23	-0.41	-0.45	-0.36

ACKNOWLEDGMENT

This work is supported by Synchronous Condenser Application (SCAPP) project funded by ForskEL program, grant no. 12196 administrated by Energinet.dk.

REFERENCES

[1] P. Tielens and D. V. Hertem, "The relevance of inertia in power systems," *Renew. Sustain. Energy Rev.*, vol. 55, pp. 999-1009, Mar. 2016.
[2] Nordic TSOs, "Challenges and opportunities for the Nordic power system," pp. 1-66, 2016. [online]. Available: http://www.svk.se/en/about-us/news/european-electricity-market/report-challenges-and-opportunities-for-the-nordic-power-system/
[3] A. Ulbig, T. S. Borsche, and G. Andersson, "Impact of low inertia on power system stability and operation," *presented at IFAC World Congress 2014*, Capetown, South Africa, Dec. 2014
[4] NERC, "1200 MW fault induced solar photovoltaic resource interruption disturbance," Jun. 2017. [online]. Available: http://www.nerc.com
[5] F. Díaz-González, M. Hau, A. Sumper, and O. Gomis-Bellmunt, "Participation of wind power plants in system frequency control: Review of grid code requirements and control methods," *Renew. Sustain. Energy Rev.*, vol. 34, pp. 551–564, Apr. 2014.
[6] F. Teng and G. Strbac, "Assessment of the role and value of frequency response support from wind plants," *IEEE Trans. Sustain. Energy*, vol. 7, no. 2, pp. 586–595, Apr. 2016.
[7] M. Kayikçi and J. V. Milanović, "Dynamic contribution of DFIG-based wind plants to system frequency disturbances," *IEEE Trans. Power Syst.*, vol. 24, no. 2, pp. 859–867, May 2009.
[8] J. Hu, L. Sun, X. Yuan, S. Wang, and Y.-N. Chi, "Modeling of type 3 wind turbine with df/dt inertia control for system frequency response study," *IEEE Trans. Power Syst.*, vol. 32, no. 4, pp. 2799–2809, Oct. 2016.
[9] J. V. D. Vyver, J. D. M. D. Kooning, B. Meersman, L. Vandevelde, and T. L. Vandoorn, "Droop control as an alternative inertial response strategy for the synthetic inertia on wind turbines," *IEEE Trans. Power Syst.*, vol. 31, no. 2, pp. 1129–1138, Mar. 2016.
[10] M. Wang-Hansen, R. Josefsson, and H. Mehmedovic, "Frequency controlling wind power modeling of control strategies," *IEEE Trans. Sustain. Energy*, vol. 4, no. 4, pp. 954–959, Oct. 2013.
[11] J. M. Mauricio, A. Marano, A. Gomez-Exposito, and J. L. Martinez Ramos, "Frequency regulation contribution through variable-speed wind energy conversion systems," *IEEE Trans. Power Syst.*, vol. 24, no. 1, pp. 173–180, Feb. 2009.
[12] G. C. Tarnowski, "Coordinated frequency control of wind turbines in power systems with high wind power penetration," Ph.D. dissertation, Dept. Elec. Eng., Tech. Univ. Denmark, Lyngby, 2011.
[13] F. M. Gonzlez-Longatt, "Activation schemes for synthetic inertia controller on wind turbines based on full rated converter," in *Proc. IEEE PowerTech 2015*, Eindhoven, Netherlands, Jun. 29-Jul. 2, 2015, pp. 1-5.
[14] N. Mendis, K. M. Muttaqi, and S. Perera, "Management of battery-supercapacitor hybrid energy storage and synchronous condenser for isolated operation of PMSG based variable-speed wind turbine generating systems," *IEEE Trans. Smart Grid*, vol. 5, no. 2, pp. 944–953, Mar. 2014.
[15] Siemens, "The stable way synchronous condenser solutions," 2014. [online]. Available:http://www.energy.siemens.com/ru/pool/hq/power-transmission/FACTS/Synchronous-Condenser/Synchronous-Condenser.pdf
[16] N. A. Masood, R. Yan, T. K. Saha, and N. Modi, "Frequency response and its enhancement using synchronous condensers in presence of high wind penetration," in *Proc. 2015 IEEE Power and Energy Society General Meeting*, Denver, CO, Jul. 26-30, 2015, pp. 1-5.
[17] A. Moeini and I. Kamwa, "Analytical concepts for reactive power base primary frequency control in power systems," *IEEE Trans. Power Syst.*, vol. 31, no. 6, pp. 4217-4230, Nov. 2016.
[18] Y. J. Kim and J. Wang, "Power hardware-in-the-loop simulation study on frequency regulation through direct load control of thermal and electrical energy storage resources," *IEEE Trans. Smart Grid*, vol. PP, no. 99, pp. 1-10, 2017.
[19] F. Alvarez-Gonzalez, A. Griffo, B. Sen, and J. Wang, "Real-time hardware-in-the-loop simulation of permanent magnet synchronous motor drives under stator faults," *IEEE Trans. Industrial Electronics*, vol. PP, no. 99, pp. 1-10, Mar. 2017.
[20] H. T. Nguyen, G. Y. Yang, A. H. Nielsen, and P. H. Jensen, "Frequency stability improvement of low inertia systems using synchronous condensers," in *Proc. 2016 IEEE International Conference on Smart Grid Communications*, Sydney, Australia, Nov. 6-9, 2016.
[21] *Frequency stability Evaluation criteria for the synchronous zone of continental Europe*, ENTSO-E, Brussels, Belgium, Mar. 2016.

This article has been accepted for publication in a future issue of this journal, but has not been fully edited. Content may change prior to final publication. Citation information: DOI 10.1109/TSTE.2018.2856938, IEEE Transactions on Sustainable Energy

[22] *The load-frequency and reserves network code*, ENTSO-E, Brussels, Belgium, Jan. 2013.
[23] D. Kosterev, "Load modeling in power system studies: WECC progress update," in *Proc. 2008 IEEE Power and Energy Society General Meeting*, Pittsburgh, PA, Jul. 20-24, 2008, pp. 1-8.
[24] A. R. Khatib, M. Appannagari, S. Manson and S. Goodall, "Load modeling assumptions: what is accurate enough?," *IEEE Trans. Ind. App.*, vol. 52, no. 4, pp. 3611-3619, July-Aug. 2016.
[25] *ENTSO-E network code for requirements for grid connection applicable to all generators*, ENTSO-E, Brussels, Belgium, 2013. [online]. Available: https://www.entsoe.eu/
[26] H. T. Nguyen, G. Y. Yang, A. H. Nielsen, and P. H. Jensen, "Frequency stability Enhancement of low inertia systems using synthetic inertia," in *Proc. 2017 IEEE Power and Energy Society General Meeting*, Chicago, IL, Jul. 16-21, 2017, pp. 1-5.
[27] ELFORSK, "Report of Vindforsk Project V-369," Jan. 2013. [online]. Available: http://www.elforsk.se/Programomraden/El-Varme/Vindforsk/reports/reports-VFIII

Ha Thi Nguyen received the B.Sc. and M.Sc. degrees in electric power system from University of Science and Technology - the University of Danang, Vietnam, 2010, and National Cheng Kung University, Taiwan, 2014, respectively. In 2014, she was a lecturer at Department of Electrical Engineering, University of Science and Technology - the University of Danang, Vietnam. She is currently pursuing her Ph.D. degree in the Center for Electric Power and Energy, Department of Electrical Engineering, Technical University of Denmark, Kgs. Lyngby, Denmark. In 2017, she was a visiting Scholar at the Centre Energy Research, University of California San Diego, California, USA. Her research interests are power system simulation and control, frequency stability and control, and renewable energy.

Guangya Yang received the B.E., M.E., and Ph.D. degrees all in the field of electric power system, in 2002, 2005, and 2008, respectively. Since 2009, he has been with the Technical University of Denmark, Kongens Lyngby, Denmark, as a Postdoctoral Researcher, and he is currently an Associate Professor with the Center for Electric Power and Energy, Department of Electrical Engineering, Technical University of Denmark. Since 2009, he has been leading several industrial collaborative projects in Denmark in the field of monitoring, operation and protection of renewable energy systems. His research interests include renewable energy integration, smart grids, and cyber-physical energy systems

Arne Hejde Nielsen is an Associate Professor at the Centre for Electric Power and Energy, Department of Electrical Engineering, Technical University of Denmark, Kongens Lyngby, Denmark. He has 30 years experience in electric power engineering; the first years were from ASEA AB, Central Research and Development Department, Sweden, with focus on measurement technology and motor design and control. Over the past decade, his focus has been on electric power systems, especially on the implementation of renewable energy sources in the power system.

Peter Højgaard Jensen is a System Specialist at Siemens A/S. He received the M.Sc. degree in electrical engineering from the Technical University of Denmark, Lyngby in 1979. He has 34 years' experience from Danish Power Plants in maintenance, operation, management, engineering, power plant erection and commissioning. Five years in Siemens have been used for developing new control concept for Synchronous Condensers (SynCon's) and commissioning of 13 SynCon's in Denmark, Norway, Texas and California (175-270 MVAr).